

# PANIC-ATTAC: A Mouse Model for Inducible and Reversible $\beta$ -Cell Ablation

Zhao V. Wang,<sup>1,2,3</sup> James Mu,<sup>4</sup> Todd D. Schraw,<sup>2,3</sup> Laurent Gautron,<sup>2,5,6</sup> Joel K. Elmquist,<sup>2,5,6</sup> Bei B. Zhang,<sup>4</sup> Michael Brownlee,<sup>7</sup> and Philipp E. Scherer<sup>2,3</sup>

**OBJECTIVE**—Islet transplantations have been performed clinically, but their practical applications are limited. An extensive effort has been made toward the identification of pancreatic  $\beta$ -cell stem cells that has yielded many insights to date, yet targeted reconstitution of  $\beta$ -cell mass remains elusive. Here, we present a mouse model for inducible and reversible ablation of pancreatic  $\beta$ -cells named the PANIC-ATTAC (pancreatic islet  $\beta$ -cell apoptosis through targeted activation of caspase 8) mouse.

**RESEARCH DESIGN AND METHODS**—We efficiently induce  $\beta$ -cell death through apoptosis and concomitant hyperglycemia by administration of a chemical dimerizer to the transgenic mice. In contrast to animals administered streptozotocin, the diabetes phenotype and  $\beta$ -cell loss are fully reversible in the PANIC-ATTAC mice, and we find significant  $\beta$ -cell recovery with normalization of glucose levels after 2 months.

**RESULTS**—The rate of recovery can be enhanced by various pharmacological interventions with agents acting on the glucagon-like peptide 1 axis and agonists of peroxisome proliferator-activated receptor- $\gamma$ . During recovery, we find an increased population of GLUT2<sup>+</sup>/insulin<sup>-</sup> cells in the islets of PANIC-ATTAC mice, which may represent a novel pool of potential  $\beta$ -cell precursors.

**CONCLUSIONS**—The PANIC-ATTAC mouse may be used as an animal model of inducible and reversible  $\beta$ -cell ablation and therefore has applications in many areas of diabetes research that include identification of  $\beta$ -cell precursors, evaluation of glucotoxicity effects in diabetes, and examination of pharmacological interventions. *Diabetes* 57:2137–2148, 2008

**D**iabetes is an epidemic affecting 180 million people worldwide with rising prevalence (1). Successful islet transplantation with the Edmonton protocol was considered a significant step toward a cure (2). However, because of the scarcity of available islets and limited viability of transplanted islets,

From the <sup>1</sup>Department of Cell Biology, Albert Einstein College of Medicine, Bronx, New York; the <sup>2</sup>Department of Internal Medicine, University of Texas Southwestern Medical Center, Dallas, Texas; the <sup>3</sup>Touchstone Diabetes Center, University of Texas Southwestern Medical Center, Dallas, Texas; the <sup>4</sup>Department of Metabolic Disorders, Merck Research Laboratories, Rahway, New Jersey; the <sup>5</sup>Department of Pharmacology, University of Texas Southwestern Medical Center, Dallas, Texas; the <sup>6</sup>Division of Hypothalamic Research, University of Texas Southwestern Medical Center, Dallas, Texas; and the <sup>7</sup>Department of Medicine and Diabetes Research Center, Albert Einstein College of Medicine, Bronx, New York.  
Corresponding author: Philipp E. Scherer, philipp.scherer@utsouthwestern.edu.

Received 21 November 2007 and accepted 5 May 2008.  
Published ahead of print at <http://diabetes.diabetesjournals.org> on 9 May 2008.  
DOI: 10.2337/db07-1631.

© 2008 by the American Diabetes Association. Readers may use this article as long as the work is properly cited, the use is educational and not for profit, and the work is not altered. See <http://creativecommons.org/licenses/by-nc-nd/3.0/> for details.

The costs of publication of this article were defrayed in part by the payment of page charges. This article must therefore be hereby marked "advertisement" in accordance with 18 U.S.C. Section 1734 solely to indicate this fact.

this procedure has not yet found widespread application. Extensive efforts have been directed toward identifying pancreatic  $\beta$ -cell stem cells for transplantation and approaches to stimulate  $\beta$ -cell regeneration.

In the past, the potential  $\beta$ -cell precursors have been identified among embryonic stem cells, ductal cells, acinar cells, and nonendocrine epithelial cells (3–7). More recently, the proliferation of pre-existing  $\beta$ -cells has been shown to be the major source of  $\beta$ -cell regeneration in lineage tracing studies (8). The mechanisms of  $\beta$ -cell regeneration therefore remain controversial, and different methodologies and animal models may be at the source of these inconsistent observations.

Both in vitro islet culture and diabetic animal models have been used extensively in characterization of pancreatic  $\beta$ -cell death and regeneration and identification of  $\beta$ -cell precursors. However, the findings gained from islet cultures in vitro cannot always be extrapolated to the in vivo situation because of the complexity of  $\beta$ -cell physiology. Current in vivo pancreas injury models include toxin administration, pancreatectomy, and ductal ligation. Studies using these models have provided valuable insights for physiological and pathophysiological regulation of  $\beta$ -cells. However, these animal models use acute, extreme, and nonphysiological insults, and none of them show significant  $\beta$ -cell recovery after injury.

In the present study, we describe a pancreas injury model with inducible and reversible  $\beta$ -cell ablation. In the current transgenic mouse model, the PANIC-ATTAC (pancreatic islet  $\beta$ -cell apoptosis through targeted activation of caspase 8) mouse,  $\beta$ -cell death is induced in a specific and well-defined manner through treatment of a chemical dimerizer. Importantly, the PANIC-ATTAC mice show extensive  $\beta$ -cell regeneration and normalization of glucose levels after treatment. We found an increased population of GLUT2<sup>+</sup>/insulin<sup>-</sup> cells, which may serve as  $\beta$ -cell precursors. The PANIC-ATTAC mouse model has the potential to be highly informative in many areas of diabetes research and provides an opportunity to characterize  $\beta$ -cell pathophysiology during diabetes progression.

## RESEARCH DESIGN AND METHODS

**Generation of the PANIC-ATTAC transgenic mice.** The rat insulin promoter was used to drive the expression of FKBP–caspase 8 fusion protein. A PCR fragment containing FKBP–caspase 8 and 3'-untranslated region was cloned into pCR4TA (Invitrogen) and then subcloned into the promoter vector. After linearization, the DNA preparation was injected into FVB embryos. Positive lines were identified by PCR genotyping (9). All animal protocols were approved either by the Institute for Animal Studies of the Albert Einstein College of Medicine or by the Institutional Animal Care and Use Committee of University of Texas Southwestern Medical Center at Dallas.

**Tests and assays.** For oral glucose tolerance test (OGTT), mice were fasted for 2.5 h before glucose oral gavage at 2.5 mg/kg body wt. Tail blood was drawn for glucose measurements by an oxidase-peroxidase assay (Sigma). The insulin levels were determined by an insulin ELISA assay (Millipore). For

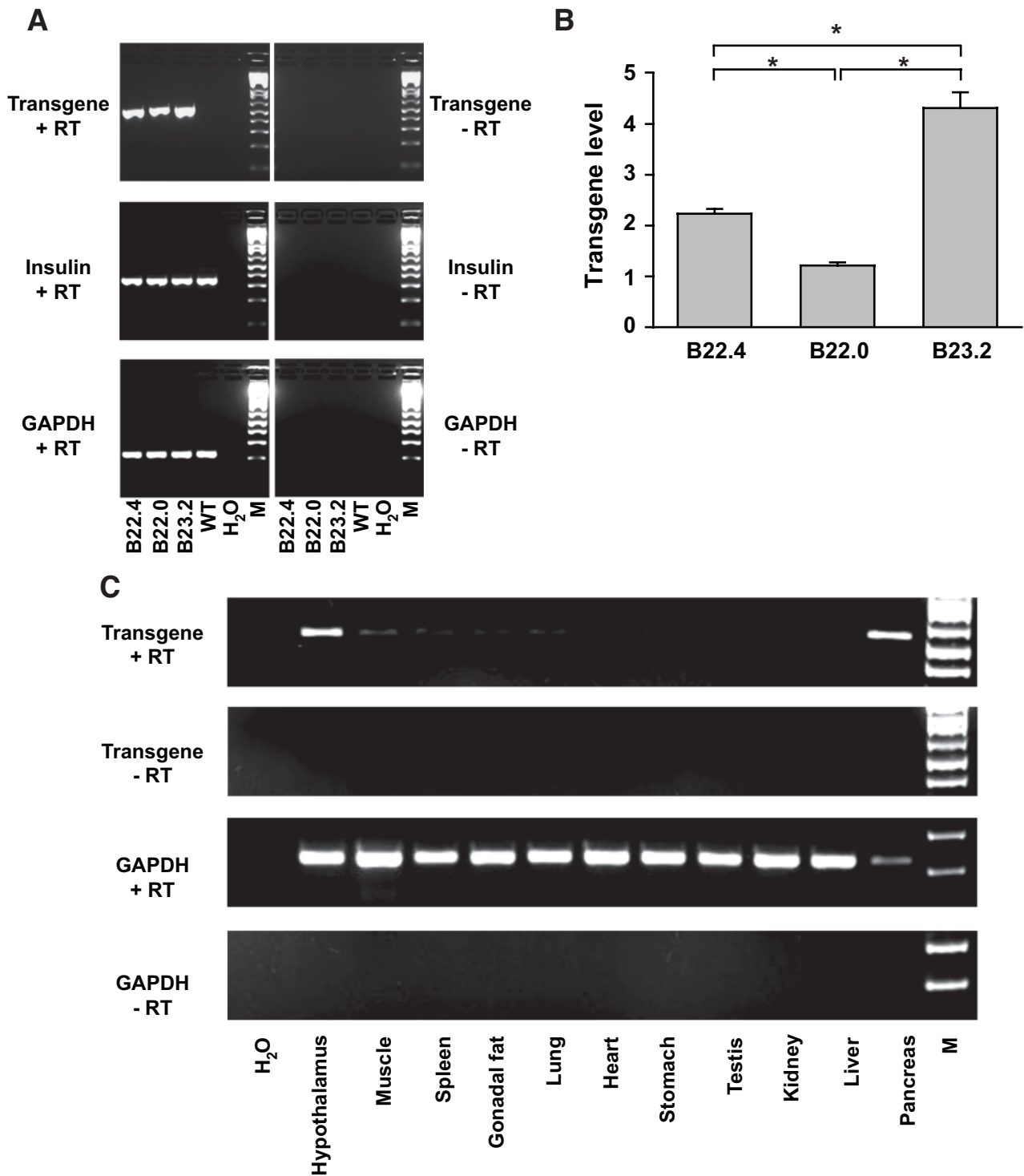


**FIG. 1.** Generation of PANIC-ATTAC transgenic mice. **A:** Transgene expression in all the three founder transgenic lines. Total RNA from whole pancreas was isolated and processed for reverse transcription. The PCR amplification results are shown for the transgene, insulin, and GAPDH, with the latter two as loading controls. **B:** Quantitative PCR analysis to determine the expression levels of the transgene relative to insulin in three positive founder lines.  $n = 5$  per mouse line.  $*P < 0.001$ . **C:** Tissue distribution of the transgene in the founder line B23.2. GAPDH was used as a loading control. Note that the relative expression of transgene in pancreas is higher compared with hypothalamus due to the partial degradation of RNA during preparation indicated by the low GAPDH signal in the pancreas.

intraperitoneal glucose tolerance tests (IPGTTs), mice were fasted for 5 h, and glucose was administrated at a concentration of 2.5 mg/kg body wt. The pancreatic insulin content was measured as described previously (10). For insulin tolerance tests (ITTs), mice were fasted for 2.5 h before administration of insulin at 1 IU/kg body wt intraperitoneally (Novo Nordisk). **Dimerizer administration.** The dimerizer AP20187 was administrated to 2- to 3-month-old animals according to the manufacturer's recommendations (Ariad Pharmaceuticals). For hemizygous PANIC-ATTAC mice, dimerizer of

0.2  $\mu$ g/g body wt was injected twice a day at 12:00 P.M. and 6:00 P.M. every other day for a total of eight injections. For homozygous PANIC-ATTAC mice, a single injection (0.2 or 0.3  $\mu$ g/g body wt) was performed at 12:00 P.M. **Histology.** Pancreata were dissected and fixed in 10% buffered formalin overnight. Paraffin sections of 5  $\mu$ m were processed for histology. For immunofluorescence, sections were incubated with primary antibodies for 24 h and subsequently decorated with secondary antibodies for 1 h at room temperature. Antibodies used include guinea pig anti-swine insulin (1:500;

DAKO), rabbit anti-human glucagon (1:250; Zymed), rabbit anti-GLUT2 (1:200; Chemicon), rabbit anti-PDX-1 (1:200; provided by Dr. Raymond MacDonald), goat anti-PDX-1 (1:1,000; provided by Dr. Klaus Kaestner), rat anti-mouse Ki67 (1:100; DAKO), rabbit anti-MafA (1:1,000; Bethyl Labs), donkey anti-guinea pig IgG-fluorescein isothiocyanate (1:250; Jackson Immunoresearch), and donkey anti-rabbit IgG-Cy3 (1:500; Jackson Immunoresearch). Images were taken on a Leica TCS SP5 confocal microscope. For immunohistochemistry, sections were incubated with primary antibodies for 24 h at 4°C. Sections were then incubated with biotinylated secondary antibodies (1:500 anti-guinea pig IgG and 1:200 anti-rabbit IgG [DAKO]) for 1 h at room temperature, and reaction was developed with ABC reagent (Vector Laboratories). Images were acquired with Coolscope (Nikon). To visualize apoptotic nuclei, transferase-mediated dUTP nick-end labeling (TUNEL) staining was performed using an *in situ* cell death detection kit (Roche) (11). To measure  $\beta$ -cell mass, a full-print pancreas section was chosen for immunostaining of insulin. The whole area of the pancreas was calculated by ImageJ. The sum area of all islets was calculated with the automatic measurement tool of AxioVision 4.6 (Carl Zeiss). To study the role of the hypothalamus, mice were perfused with 10% formalin, and the brain was removed for overnight fixation. After 24-h incubation in 20% sucrose, hypothalamus free-floating sections (25  $\mu$ m) were produced using a freezing microtome. Hypothalamus sections were mounted on glass slides, air dried, and processed for TUNEL staining.

**Treatments.** For streptozotocin (STZ) administration, FVB mice received a single intraperitoneal dose (175 mg/kg) of freshly prepared STZ (Sigma). For Exendin-4 administration, male hemizygous transgenic PANIC-ATTAC mice were fed with high-fat diet 4 weeks before hyperglycemic induction. Two doses of exendin-4, 3.3 or 10  $\mu$ g/kg body wt ( $\mu$ pk), were selected for daily injection at 4:00 P.M. Postprandial glucose and body weight were monitored periodically. For peroxisome proliferator-activated receptor (PPAR)- $\gamma$  agonist administration, the 2-(2-(4-phenoxy-2-propylphenoxy)ethyl)indole-5-acetic acid compound, a gift from Merck Research Laboratories (12), was mixed with powdered food at 75  $\mu$ g/g. The average dose for mice is 10 mg/kg body wt. For the sitagliptin studies (13), male homozygous PANIC-ATTAC mice were induced to hyperglycemia by three continuous injections of dimerizer (0.2  $\mu$ g/g body wt) 24 h apart and put on diet mixed with compound (7.8 g active ingredient/kg chow diet) (Research Diets). Postprandial glucose and body wt were monitored periodically. An OGTT was conducted at day 75 of sitagliptin treatment. Serum samples obtained from terminal bleeds (postprandial) at day 80 were used for active glucagon-like peptide 1 (GLP-1) level determination using an active GLP-1 ELISA assay (Millipore).

**Statistical analysis.** Results were presented as means  $\pm$  SE. Statistical analysis was performed with the Student's *t* test except OGTT, IIT, and glucose profiling results, which were done by two-way ANOVA and subsequent Tukey's test. Significance was accepted at  $P < 0.05$ .

## RESULTS

**Generation of transgenic PANIC-ATTAC mice.** To ablate pancreatic  $\beta$ -cells in a targeted and inducible way, we have taken advantage of the cell-specific expression of a FKBP-caspase 8 fusion protein. This approach relies on a system developed by Clackson et al. (14) that uses a mutated form of FKBP domain which selectively and avidly binds a FK506 analog but not the endogenous ligand. This interaction can bring two mutant FKBP domains in close proximity, thereby effectively inducing dimerization of any passenger protein attached to the FKBP moiety. We fused the mutant FKBP domain to caspase 8, which can lead to apoptosis after dimerization (15). The expression of this FKBP-caspase 8 protein does not convey a phenotype in its monomeric form. However, on administration of a chemical that forces the dimerization of caspase 8 through interaction with the FKBP domain, caspase 8 is activated, and the apoptotic cascade is initiated (16). We have previously described a mouse model that carries such a transgene under the control of an adipocyte-specific promoter (fat apoptosis through targeted activation of caspase 8 [FAT-ATTAC]) in which we were able to inducibly ablate adipocytes (9). Here, we put the gene encoding this fusion protein under the control of the rat insulin promoter. By RT-PCR analysis, we found that all three lines expressed the transgene (Fig. 1A). By

quantitative PCR, line B23.2 showed the highest expression and was chosen for further studies (Fig. 1B). We refer to this mouse model as PANIC-ATTAC.

To evaluate tissue-specific expression, RT-PCR analysis was performed on 11 tissues of a transgenic mouse. As expected, the pancreas showed high level expression (Fig. 1C). Several reports in the literature have indicated that the rat insulin promoter cassette can convey expression in the brain, which is consistent with what we found here (17). Expression can be seen in a number of regions (S. Chua, personal communication; data not shown). Importantly, however, activation of the hypothalamic caspase 8 does not seem to occur under conditions when the pancreatic  $\beta$ -cells are efficiently ablated because no evidence of apoptosis in hypothalamic neurons could be found under these conditions (supplementary Fig. 1, available in an online appendix [available at <http://dx.doi.org/10.2337/db07-1631>]). This could be due to the resistance of neurons to caspase-8-mediated apoptosis or to the inability of the dimerizer compound to effectively cross the blood-brain barrier. We were unable to trigger neuronal apoptosis even after direct intracerebroventricular administration of the dimerizer (not shown). We therefore believe that it is very unlikely that the effects reported below would be influenced by events triggered in the brain on dimerizer treatment.

**Characterization of mice hemizygous for the PANIC-ATTAC transgene.** Wild-type and transgenic mice are phenotypically indistinguishable for body weight (data not shown), glucose and insulin levels during OGTT, pancreatic insulin content, and islet architecture (Fig. 2A). We concluded that the mice had no measurable baseline phenotype.

A cohort of wild-type and transgenic animals was chosen for treatment with the dimerizer compound of eight injections. An OGTT was performed 8 days after the initiation of treatment. Interestingly, despite identical genetic background and treatment regimen, the transgenic mice could be grouped into low responders, whose glucose levels were elevated but still  $<300$  mg/dl, and high responders, whose glucose levels tended to be  $>400$  mg/dl. One possible reason for this heterogeneous response may be the subtle difference of actual dimerizer delivery between animals. A similar phenomenon has been found in partial pancreatectomy animal models in which subtle variations in the proportion of pancreatic tissue removed resulted in two different degrees of hyperglycemia (18). The transgenic mice were therefore classified into two groups and analyzed separately. Both groups displayed high glucose levels during the OGTT with high responders displaying bigger excursions (Fig. 2B). None of the hyperglycemic PANIC-ATTAC animals displayed much of insulin release during OGTT. Total pancreatic insulin content was reduced by  $>75\%$  in low responders and  $>90\%$  in high responders. Correspondingly, the damage at the level of islets was quite apparent by histology. From these and other quantitative assessments of the  $\beta$ -cell mass, it is clear that hyperglycemia manifests only after a substantial portion of  $\beta$ -cell mass is eliminated (19).

We were surprised to see that on allowing these mice to recover for  $\sim 8$  weeks, the glucose tolerance during an OGTT showed improvements compared with the initial hyperglycemic conditions (Fig. 2C). Insulin release during the OGTT was, however, still impaired even though total pancreatic insulin content approached wild-type levels in the low responders and dramatically increased in the high responders. On analysis of fasting glucose levels, it is

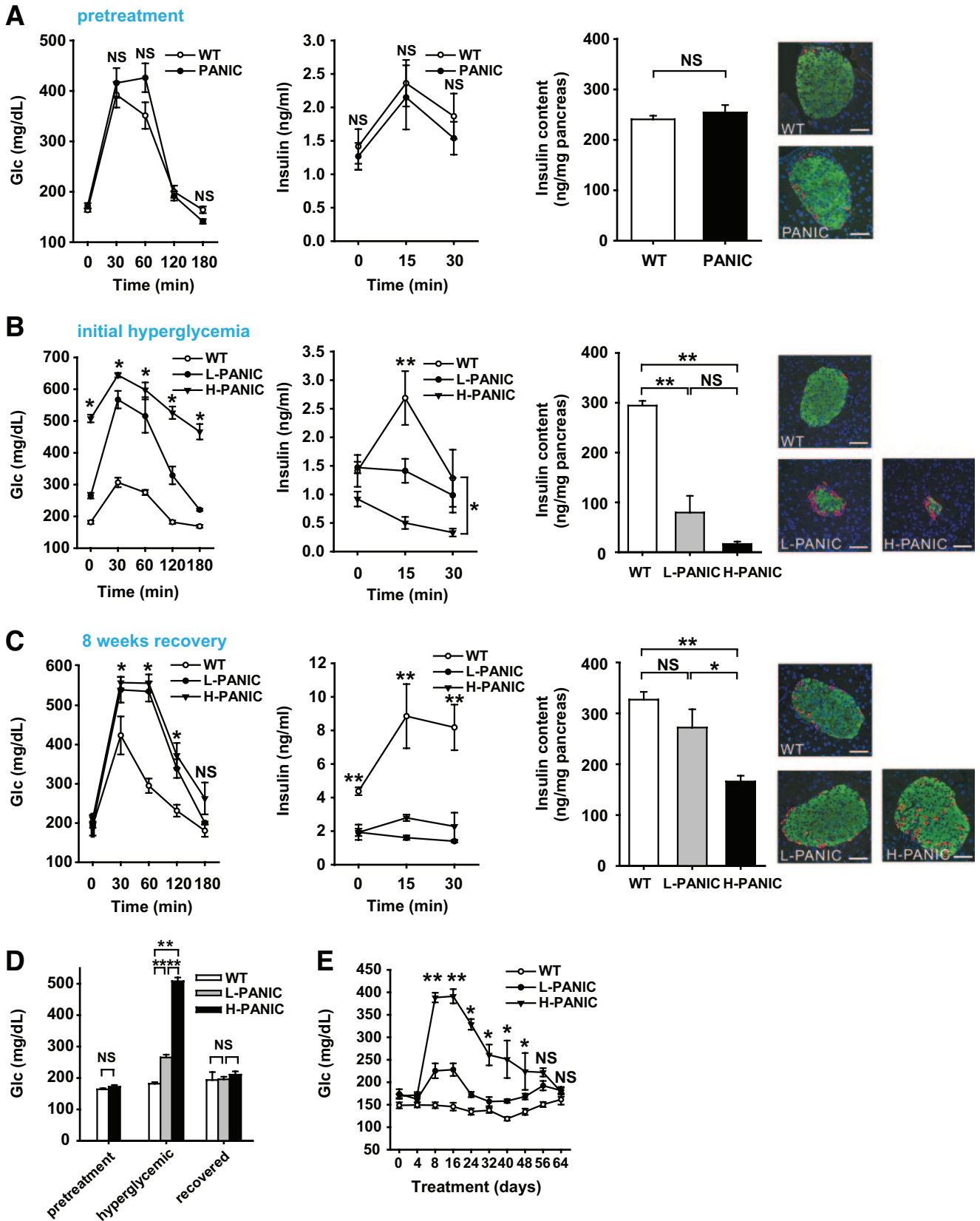


**FIG. 2.** Characterization of hemizygous PANIC-ATTAC transgenic mice. **A:** OGTT and pancreatic insulin content of wild-type and hemizygous PANIC-ATTAC mice before dimerizer administration. For OGTT,  $n = 6$  per group. For insulin content,  $n = 5$  of wild type and  $n = 4$  of PANIC-ATTAC. A representative immunofluorescent image for insulin (green), glucagon (red), and nuclei (blue) is shown. Scale bar =  $50 \mu\text{m}$ . **B:** OGTT and pancreatic insulin content of wild-type and hemizygous PANIC-ATTAC mice 8 days after administration of dimerizer (time of onset hyperglycemia). In glucose measurement during OGTT, all comparisons including wild type ( $n = 5$ ) vs. low responders (L-PANIC) ( $n = 3$ ), L-PANIC vs. high responders (H-PANIC) ( $n = 6$ ), and wild type vs. H-PANIC are statistically significant except wild type vs. L-PANIC at time 180 min. For the analysis of insulin levels during OGTT, the differences between wild type and L-PANIC at 15 min, wild type and H-PANIC at 15 min, and wild type and H-PANIC at 30 min are significant. For insulin content,  $n = 5$  of wild type,  $n = 4$  of L-PANIC, and  $n = 3$  of H-PANIC. **A**

apparent that glucose control is normalized in all mice on recovery (Fig. 2D). A more detailed analysis of fasting glucose levels during the entire period shows recovery that even the high responders manifest (Fig. 2E). These results suggest that we can effectively induce  $\beta$ -cell ablation and hyperglycemia in hemizygous PANIC-ATTAC animals and that, more importantly, the mice can restore euglycemic control after recovery.

The treatment regimen described above established the conditions under which we can obtain both low responders and high responders. We aimed to find conditions that would render the  $\beta$ -cells more susceptible to apoptosis. Lipotoxicity has been implicated in the dysfunction of  $\beta$ -cells during diabetes progression (20). When exposed to a normal chow diet, the majority of the mice convert to low responders after dimerizer treatment, with only  $\sim 30\%$  displaying a high response. On exposure to high-fat diet for 5 or 10 weeks before dimerizer treatment, a much higher percentage of mice was converted to high responders by the same injections (Fig. 3A). To assess the effects of high-fat diet on the transgene expression (under the control of rat insulin promoter II), we isolated islets and performed quantitative RT-PCR after exposure to high-fat diet. We found that high-fat diet treatment increases the transgene expression (Supplementary Fig. 2). Although transgene expression does play a role under these conditions, there may also be a contribution of lipid accumulation in  $\beta$ -cells under these conditions. The more susceptible phenotype may therefore be a combination of increased transgene expression and lipotoxicity.

**Exendin-4 treatment improves the recovery after a massive  $\beta$ -cell insult.** A number of powerful antidiabetes drugs have recently become available, many of which take advantage of the GLP-1 axis. Exendin-4 is a potent and long-lived GLP-1 receptor agonist (21) that has been shown to increase  $\beta$ -cell mass and to improve glucose tolerance (22). We chose severely challenged PANIC-ATTAC mice (glucose levels  $>500$  mg/dl) and treated them with exendin-4. As seen in Fig. 3B, dimerizer treatment and subsequent exendin-4 treatment did not have an impact on glucose levels in wild-type animals. However, PANIC-ATTAC mice that were exposed to low and high doses of exendin-4 showed a dose-dependent improvement of hyperglycemia over a period of 2 weeks. Correspondingly, the PANIC-ATTAC mice in the 10  $\mu$ g group showed lower glucose levels during an OGTT (Fig. 3C) but remained deficient in glucose-stimulated insulin secretion (GSIS) (Fig. 3D). The potent effects of exendin-4 treatment were seen when total pancreatic insulin content was measured (Fig. 3E), which was further corroborated by islet histology (Fig. 3F).

**Characterization of homozygous PANIC-ATTAC transgenic mice.** Although mice hemizygous for the PANIC-ATTAC transgene require multiple injections of dimerizer and still fall into “moderate” and “full” responder categories, we wanted to probe the effects of doubling the

transgene dosage, i.e., rendering the mice homozygous at the transgene loci. At baseline, the homozygous mice revealed no differences compared with wild-type animals (Fig. 4A). However, the higher potency of doubling transgenic dosage became apparent when a single injection of dimerizer compound at only 0.2  $\mu$ g/g body wt was sufficient to trigger a uniform response and homogeneous hyperglycemia in all mice (Fig. 4B). Phenotypically, the mice behaved as expected, with severe hyperglycemia during an OGTT, ineffective GSIS, low pancreatic insulin content, and very few insulin<sup>+</sup> cells in islets (Fig. 4B). To confirm that the decrease of pancreatic insulin content is due to  $\beta$ -cell loss, we quantified the  $\beta$ -cell mass 8 days after initiation of dimerizer treatment. We detected a 10-fold decrease of  $\beta$ -cell mass, consistent with the results obtained by assessing the decrease in pancreatic insulin content (Supplementary Fig. 3). As with all models targeting  $\beta$ -cells in vivo, we cannot formally rule out the possibility of a downregulation of insulin expression in otherwise mature  $\beta$ -cells that may give a false impression of  $\beta$ -cell loss. However, the widespread apoptotic  $\beta$ -cells found in islets, the absence of MafA<sup>+</sup>/insulin<sup>-</sup> cells, and the disrupted islet architecture suggest  $\beta$ -cell death is the most likely cause of decreased pancreatic insulin content and hyperglycemia. Despite the aggressive nature of the ablation, no lethality has been found, and these mice managed to mount an effective recovery as evident during an OGTT, by pancreatic insulin content, and by histology (Fig. 4C). The recovered glucose tolerance during an OGTT is accompanied by a defective insulin response. To assess whether differences in gastric absorption are involved, we performed IPGTT after 5 h of fasting. As with OGTT, we found that during IPGTT, the glucose tolerance is improved, whereas glucose-stimulated insulin secretion remains defective (Supplementary Fig. 4).

Although the initial effects shown here were obtained with a single dose of dimerizer, the homozygous mice also displayed a dose-dependent reduction of pancreatic insulin content, offering the possibility to ablate a predetermined number of  $\beta$ -cells in a reproducible and uniform manner (Fig. 4D). Focusing on the fasting glucose levels further corroborated that the mice improved their glucose control after recovery (Fig. 4E). A more refined analysis of the fasting glucose levels showed that the mice restored euglycemia within  $\sim 6$  weeks after the onset of hyperglycemia (Fig. 4F).

To formally demonstrate that the  $\beta$ -cell death triggered by forced dimerization of caspase 8 is caused by apoptosis, we performed transferase-mediated dUTP nick-end labeling (TUNEL) staining. Although relatively limited apoptosis was seen 4 h after dimerizer treatment, TUNEL<sup>+</sup> cells (red) were clearly visible 24 h after treatment, particularly in the more stringent homozygous setting (Fig. 4G). The disorganized islet structure and decreased insulin<sup>+</sup>  $\beta$ -cells in homozygous transgenic mice indicate that the peak apoptotic response may occur before 24 h,

representative immunofluorescent image for insulin (green), glucagon (red), and nuclei (blue) is shown. Scale bar = 50  $\mu$ m. \* $P < 0.05$ , \*\* $P < 0.001$ . C: OGTT and pancreatic insulin content of wild-type and hemizygous PANIC-ATTAC mice 64 days after administration of dimerizer when serum glucose returns to normal level. For glucose measurements during OGTT, the comparisons between wild type ( $n = 3$ ) versus L-PANIC ( $n = 4$ ) and wild type versus H-PANIC ( $n = 4$ ) show significant differences at 30, 60, and 120 min. For insulin measurements during OGTT, the differences between wild type ( $n = 3$ ) and L-PANIC ( $n = 3$ ) and wild type and H-PANIC ( $n = 3$ ) during the entire course are significant. For insulin content,  $n = 8$  of wild type,  $n = 4$  of L-PANIC, and  $n = 5$  of H-PANIC. A representative immunofluorescent image for insulin (green), glucagon (red), and nuclei (blue) is shown. Scale bar = 50  $\mu$ m. \* $P < 0.05$ , \*\* $P < 0.001$ . D: Fasting glucose levels of wild type, L-PANIC, and H-PANIC mice before dimerizer treatment, at the onset of hyperglycemia, and after recovery. At least three animals were recorded per group. \*\* $P < 0.001$ . E: Fasting glucose profile of wild-type ( $n = 8$ ), L-PANIC ( $n = 5$ ), and H-PANIC ( $n = 3$ ) mice during the entire recovery period. \* $P < 0.05$ , \*\* $P < 0.001$ . (Please see <http://dx.doi.org/10.2337/db07-1631> for a high-quality digital representation of this figure.)

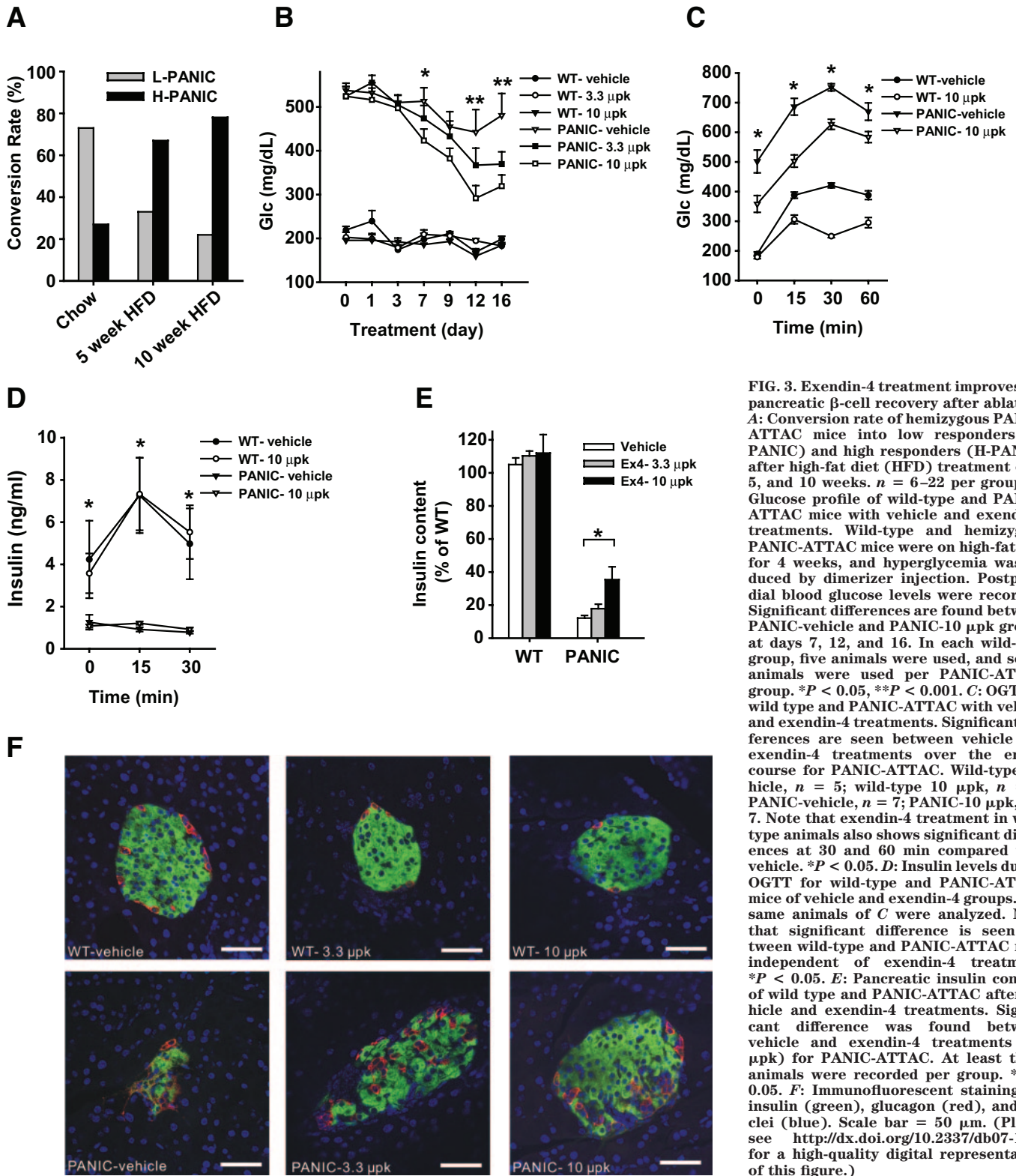
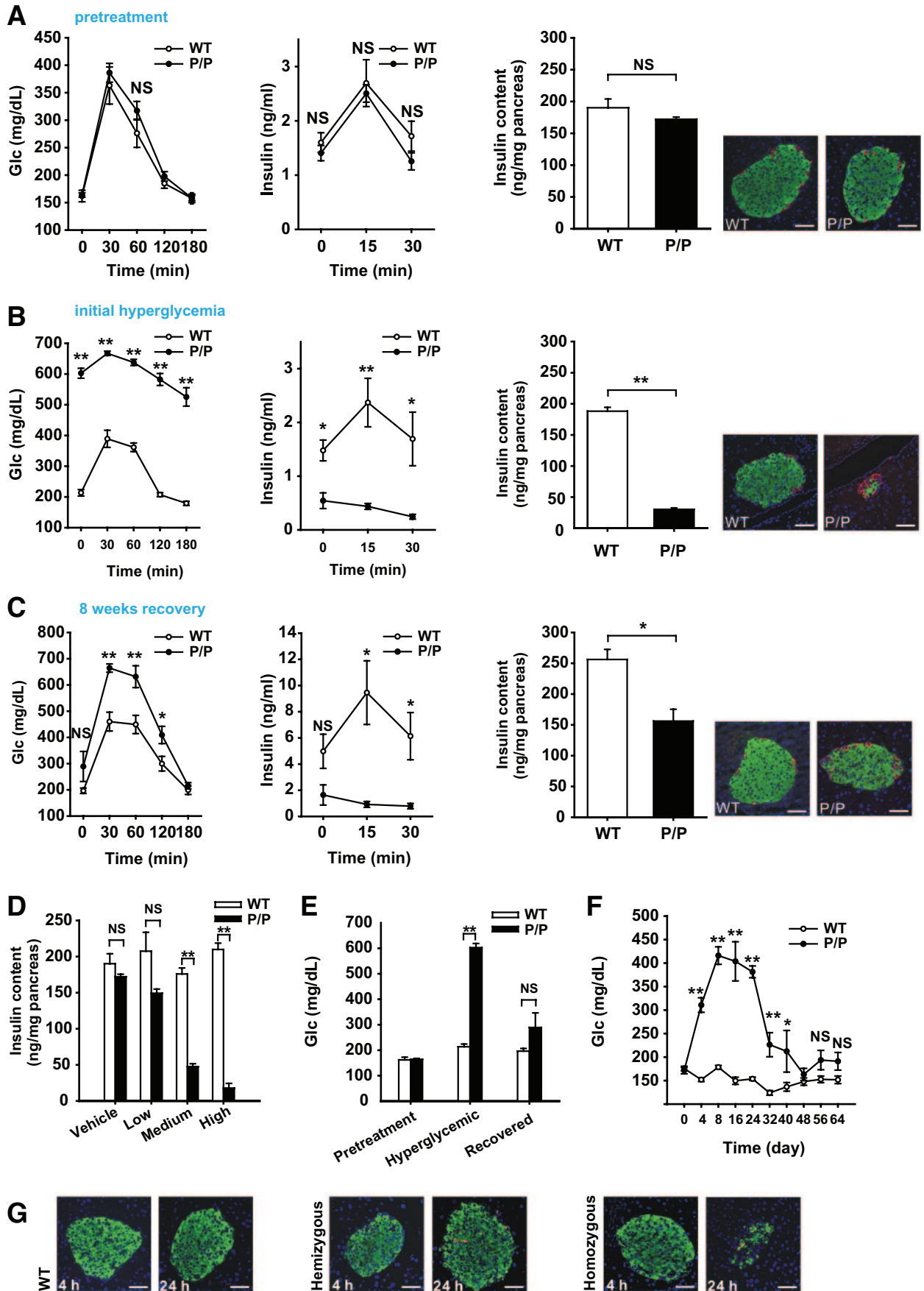


**FIG. 3.** Extensin-4 treatment improves the pancreatic  $\beta$ -cell recovery after ablation. **A:** Conversion rate of hemizygous PANIC-ATTAC mice into low responders (L-PANIC) and high responders (H-PANIC) after high-fat diet (HFD) treatment of 0, 5, and 10 weeks.  $n = 6-22$  per group. **B:** Glucose profile of wild-type and PANIC-ATTAC mice with vehicle and extensin-4 treatments. Wild-type and hemizygous PANIC-ATTAC mice were on high-fat diet for 4 weeks, and hyperglycemia was induced by dimerizer injection. Postprandial blood glucose levels were recorded. Significant differences are found between PANIC-vehicle and PANIC-10  $\mu$ pk groups at days 7, 12, and 16. In each wild-type group, five animals were used, and seven animals were used per PANIC-ATTAC group.  $*P < 0.05$ ,  $**P < 0.001$ . **C:** OGTT of wild type and PANIC-ATTAC with vehicle and extensin-4 treatments. Significant differences are seen between vehicle and extensin-4 treatments over the entire course for PANIC-ATTAC. Wild-type vehicle,  $n = 5$ ; wild-type 10  $\mu$ pk,  $n = 5$ ; PANIC-vehicle,  $n = 7$ ; PANIC-10  $\mu$ pk,  $n = 7$ . Note that extensin-4 treatment in wild-type animals also shows significant differences at 30 and 60 min compared with vehicle.  $*P < 0.05$ . **D:** Insulin levels during OGTT for wild-type and PANIC-ATTAC mice of vehicle and extensin-4 groups. The same animals of **C** were analyzed. Note that significant difference is seen between wild-type and PANIC-ATTAC mice independent of extensin-4 treatment.  $*P < 0.05$ . **E:** Pancreatic insulin content of wild type and PANIC-ATTAC after vehicle and extensin-4 treatments. Significant difference was found between vehicle and extensin-4 treatments (10  $\mu$ pk) for PANIC-ATTAC. At least three animals were recorded per group.  $*P < 0.05$ . **F:** Immunofluorescent staining for insulin (green), glucagon (red), and nuclei (blue). Scale bar = 50  $\mu$ m. (Please see <http://dx.doi.org/10.2337/db07-1631> for a high-quality digital representation of this figure.)

whereas in hemizygous mice, the normal appearance of islets with a sharp increase of apoptotic staining suggests that massive  $\beta$ -cell death is about to initiate at 24 h after treatment.

**PPAR- $\gamma$  agonist and sitagliptin treatments improve  $\beta$ -cell recovery in homozygous PANIC-ATTAC mice.** The stimulation of the GLP-1 axis is a powerful approach to speed up recovery in the hemizygous PANIC-ATTAC mice. Although a  $\beta$ -cell-specific PPAR- $\gamma$

knockout only showed a relatively mild phenotype (23), recent studies suggested that PPAR- $\gamma$  can in fact play an important role in  $\beta$ -cell physiology (24). To probe whether PPAR- $\gamma$  agonists may have an impact on recovery, homozygous PANIC-ATTAC mice were treated with a single dose of dimerizer at 0.3  $\mu$ g/g body wt to trigger severe hyperglycemia. On day 8 after dimerizer treatment, mice were treated with a PPAR- $\gamma$  agonist (COOH) (12). By day 28, fasting glucose had nearly recovered to



Downloaded from <http://diabetesjournals.org/diabetes/article-pdf/57/8/2137/391345/zd00808002137.pdf> by guest on 05 October 2022

Caption on following page

baseline levels (Fig. 5A). The OGTT response also improved significantly (Fig. 5B), but GSIS remained impaired (Fig. 5C). Although PPAR- $\gamma$  agonists have a potent impact on insulin sensitivity in peripheral tissues, they also have an effect on  $\beta$ -cells by increasing the pancreatic insulin content, even though the differences did not reach statistical significance (Fig. 5D). An ITT on day 48 revealed only modest differences between PPAR- $\gamma$  agonist and vehicle treatments (Fig. 5E). Whether the improvements found in glucose control are a function of direct effects of PPAR- $\gamma$  in  $\beta$ -cells or reflect an indirect mechanism of action of PPAR- $\gamma$  agonist action in adipocytes or other tissues remains to be seen.

Sitagliptin is a dipeptidyl peptidase-4 inhibitor in clinical use, increasing active GLP-1 levels (10,13). After induction of severe hyperglycemia, sitagliptin treatment was initialized as a food additive. We found that the active GLP-1 levels were increased twofold in sitagliptin-treated animals (Fig. 5F). This was accompanied by an improved glucose tolerance (Fig. 5G) and substantial restoration of islet structure and morphology (Fig. 5H) (10).

**PANIC-ATTAC mice display improved insulin sensitivity on recovery.** An additional interesting phenomenon was unraveled when we assessed the recovered transgenic mice. Because they had undergone several weeks of hyperglycemia, we expected that the chronic exposure to high glucose would have caused permanent damage due to a “hyperglycemic memory” effect leading to insulin resistance. However, we found that recovered PANIC-ATTAC mice displayed significant improvements in insulin sensitivity in both hemizygous (Fig. 6A) and homozygous mice (Fig. 6B). Although the low concentrations of available insulin may contribute to the increased effectiveness of injected insulin, there may be additional mechanisms in place in light of the rather unusual but physiological context in which the PANIC-ATTAC animals operate.

**GLUT2<sup>+</sup>/insulin<sup>-</sup> cell number increases after  $\beta$ -cell recovery.** The remarkable recovery of pancreatic  $\beta$ -cells in PANIC-ATTAC mice raises the question of what cell type gives rise to the newly emerging  $\beta$ -cell population. On careful analysis of the recovering pancreas, insulin<sup>+</sup> cells appeared in the ducts (data not shown), which has been suggested to be a sign for  $\beta$ -cell neogenesis (4,25). However, we decided to focus on a different cell type that may or may not be related to the insulin<sup>+</sup> ductal cells. We took advantage of the fact that animals administered high-dose STZ generally do not recover from hyperglycemia (Fig. 6C compared with Fig. 4F). The main route of cellular entry of STZ is through the glucose transporter GLUT2 (26). We reasoned that high-dose STZ administration results in

irreversible damage to the pancreas because  $\beta$ -cell precursors may also express GLUT2 and the lack of recovery is mostly due to simultaneous elimination of both adult  $\beta$ -cells and precursors. In the PANIC-ATTAC mice, we are ablating only mature, insulin<sup>+</sup>  $\beta$ -cells. If this is the case, we postulated that we should be able to identify a novel population of insulin<sup>-</sup>/GLUT2<sup>+</sup> cells in the recovering PANIC-ATTAC mice. This is the case (Fig. 6D). Although in wild-type cells, GLUT2 staining is restricted to insulin<sup>+</sup> cells with very few GLUT2<sup>+</sup>/insulin<sup>-</sup> cells, high-dose STZ administration eliminated essentially all GLUT2<sup>+</sup> cells. However, in recovering PANIC-ATTAC mice, a significant number of GLUT2<sup>+</sup> cells are insulin<sup>-</sup> and PDX-1<sup>-</sup> (Fig. 6D; Supplementary Fig. 5). This is suggestive that a  $\beta$ -cell precursor pool exists that is defined by GLUT2 positivity without concomitant insulin expression. We are currently in the process of developing an approach to isolate these cells. Further characterization of these cells will have to await detailed lineage tracing studies.

We found that the membrane-bound localization of GLUT2 is lost in hyperglycemic PANIC-ATTAC animals compared with animals that have achieved euglycemic levels again (Fig. 6E). The predominantly intracellular localization of GLUT2 suggests that  $\beta$ -cells have additional and so far uncharacterized mechanisms in place to protect them from hyperglycemic damage that not only involves the transcriptional downregulation of GLUT2 (27) but also the intracellular retention of the transporter.

## DISCUSSION

Here, we describe a novel mouse model allowing the inducible ablation of  $\beta$ -cells at any stage during the life cycle of a mouse. Compared with several conventional pancreas injury models, the PANIC-ATTAC mice differ in a number of ways and offer great potential in several areas of islet physiology.

In the PANIC-ATTAC model, the degree of apoptosis in the  $\beta$ -cell population can be manipulated in several ways, by varying both the dose and the frequency of dimerizer treatment, by transgene dosage (hemizygous vs. homozygous animals), and by dietary intervention (high-fat diet exposure). Although an aggressive treatment regimen has the advantage of destroying a large number of  $\beta$ -cells rapidly, yielding uniform hyperglycemia, a moderate challenge can be used to examine the key anti-apoptotic responses in surviving cells.

One of the most novel aspects of this model is the dramatic recovery of  $\beta$ -cells to levels nearly identical to those before treatment. A number of mechanisms may enable the  $\beta$ -cell population to recover under these circumstances. The rather “gentle” proapoptotic approach

**FIG. 4.** Characterization of the homozygous PANIC-ATTAC mice. **A:** OGTT and pancreatic insulin content of wild-type and homozygous PANIC-ATTAC (P/P) mice before administration of dimerizer. For OGTT,  $n = 6$  per group. For pancreatic insulin content,  $n = 4$  of wild type and  $n = 3$  of P/P. A representative immunofluorescent image for insulin (green), glucagon (red), and nuclei (blue) is shown. Scale bar = 50  $\mu\text{m}$ . **B:** OGTT and pancreatic insulin content of wild-type and P/P mice 8 days after a single treatment of dimerizer. For glucose measurements during OGTT, seven animals were used per experimental group. The same animals were used for insulin analysis. For the pancreatic insulin content measurement,  $n = 6$  of wild type and  $n = 7$  of P/P. A representative immunofluorescent image for insulin (green), glucagon (red), and nuclei (blue) is shown. Scale bar = 50  $\mu\text{m}$ . \* $P < 0.05$ , \*\* $P < 0.001$ . **C:** OGTT and pancreatic insulin content of wild-type and P/P mice 64 days after administration of dimerizer. For glucose measurements during OGTT,  $n = 4$  for wild type and  $n = 3$  for P/P. Insulin measurements were performed on the same mice. For pancreatic insulin content,  $n = 5$  of wild type,  $n = 3$  of P/P. A representative immunofluorescent image for insulin (green), glucagon (red), and nuclei (blue) is shown. Scale bar = 50  $\mu\text{m}$ . \* $P < 0.05$ , \*\* $P < 0.001$ . **D:** Dose-dependent ablation of  $\beta$ -cells with dimerizer administration. Dimerizer was injected at different concentrations into wild-type and P/P animals (low, 0.05; medium, 0.2; and high, 0.5  $\mu\text{g/g}$  body wt). After 8 days, pancreatic insulin content was determined. More than three animals were recorded per treatment. \*\* $P < 0.001$ . **E:** Fasting glucose levels of wild-type and P/P mice before dimerizer treatment, at the onset of hyperglycemia (day 8), and after recovery (day 64). At least three animals were monitored in each group. \*\* $P < 0.001$ . **F:** Fasting glucose profile of wild-type and P/P animals during recovery period. More than three animals were used per group. \* $P < 0.05$ , \*\* $P < 0.001$ . **G:** Visualization of apoptotic  $\beta$ -cells by TUNEL staining in wild-type, hemizygous, and homozygous PANIC-ATTAC mice 4 and 24 h after treatment. Insulin<sup>+</sup>  $\beta$ -cells are shown in green, and apoptotic cells are shown in red. Scale bar = 50  $\mu\text{m}$ . (Please see <http://dx.doi.org/10.2337/db07-1631> for a high-quality digital representation of this figure.)

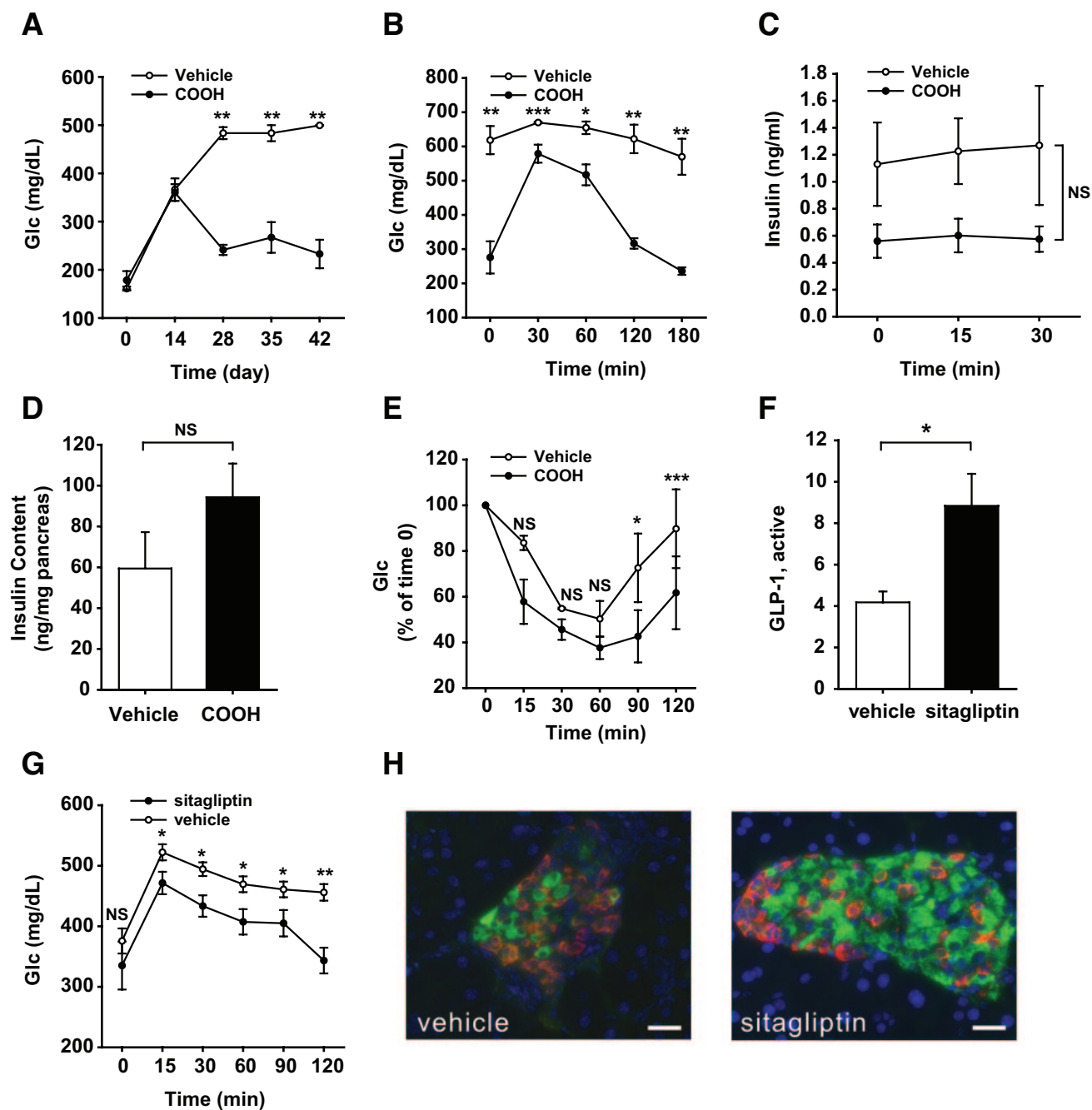


**FIG. 5.** PPAR- $\gamma$  agonist and sitagliptin treatments improve the recovery of PANIC-ATTAC mice. **A:** Fasting glucose in homozygous PANIC-ATTAC mice with vehicle and PPAR- $\gamma$  agonist (COOH) treatments. Hyperglycemia was induced by single dose of dimerizer, and the food admix treatment of COOH was initiated on day 8. Vehicle,  $n = 3$ ; COOH,  $n = 4$ .  $**P < 0.001$ . **B:** OGTT of vehicle- and COOH-treated PANIC-ATTAC mice on day 48. Vehicle,  $n = 3$ ; COOH,  $n = 4$ .  $*P < 0.05$ ,  $**P < 0.001$ ,  $***P = 0.05$ . **C:** Insulin secretion from OGTT analysis. No significant difference was found over the entire course. **D:** Pancreatic insulin content of vehicle- and COOH-treated PANIC-ATTAC mice from day 48. Vehicle,  $n = 3$ ; COOH,  $n = 4$ . **E:** ITT of vehicle- and COOH-treated PANIC-ATTAC mice on day 48. Vehicle,  $n = 4$ , COOH,  $n = 4$ .  $*P < 0.05$ ,  $***P = 0.05$ . **F:** Active GLP-1 levels are increased after sitagliptin treatment in homozygous PANIC-ATTAC mice compared with vehicle group. A total of 11 animals were recorded per group.  $*P < 0.05$ . **G:** Sitagliptin treatment improves glucose tolerance in homozygous PANIC-ATTAC mice compared with vehicle treatment. Significant differences were found at 15, 30, 60, 90, and 120 min. A total of 11 mice were used in each group.  $*P < 0.05$ ,  $**P < 0.001$ . **H:** A representative image is shown for insulin (green), glucagon (red), and nuclei (blue) of vehicle- and sitagliptin-treated homozygous PANIC-ATTAC animals. Scale bar = 50  $\mu\text{m}$ . (Please see <http://dx.doi.org/10.2337/db07-1631> for a high-quality digital representation of this figure.)

used here as opposed to the more widely used necrotic methods may minimize the inflammatory response in the islets. Hyperglycemia per se seen in the PANIC-ATTAC model may provide a more favorable environment for  $\beta$ -cell recovery compared with other pancreas injury models where hyperglycemia is usually accompanied by hyperinsulinemia and dyslipidemia. Additionally, we may preserve a potential  $\beta$ -cell precursor pool by targeting

insulin<sup>+</sup> cells compared with the less specific exposure to STZ. Similar animal models have been reported by targeting expression of diphtheria toxin specifically in  $\beta$ -cells (28,29). Nir et al. (29) found a similar phenomenon of  $\beta$ -cell regeneration after triggering ablation in their animal model, reporting results vastly consistent with the observations described here, further emphasizing the potential for plasticity of  $\beta$ -cell mass under some conditions. More

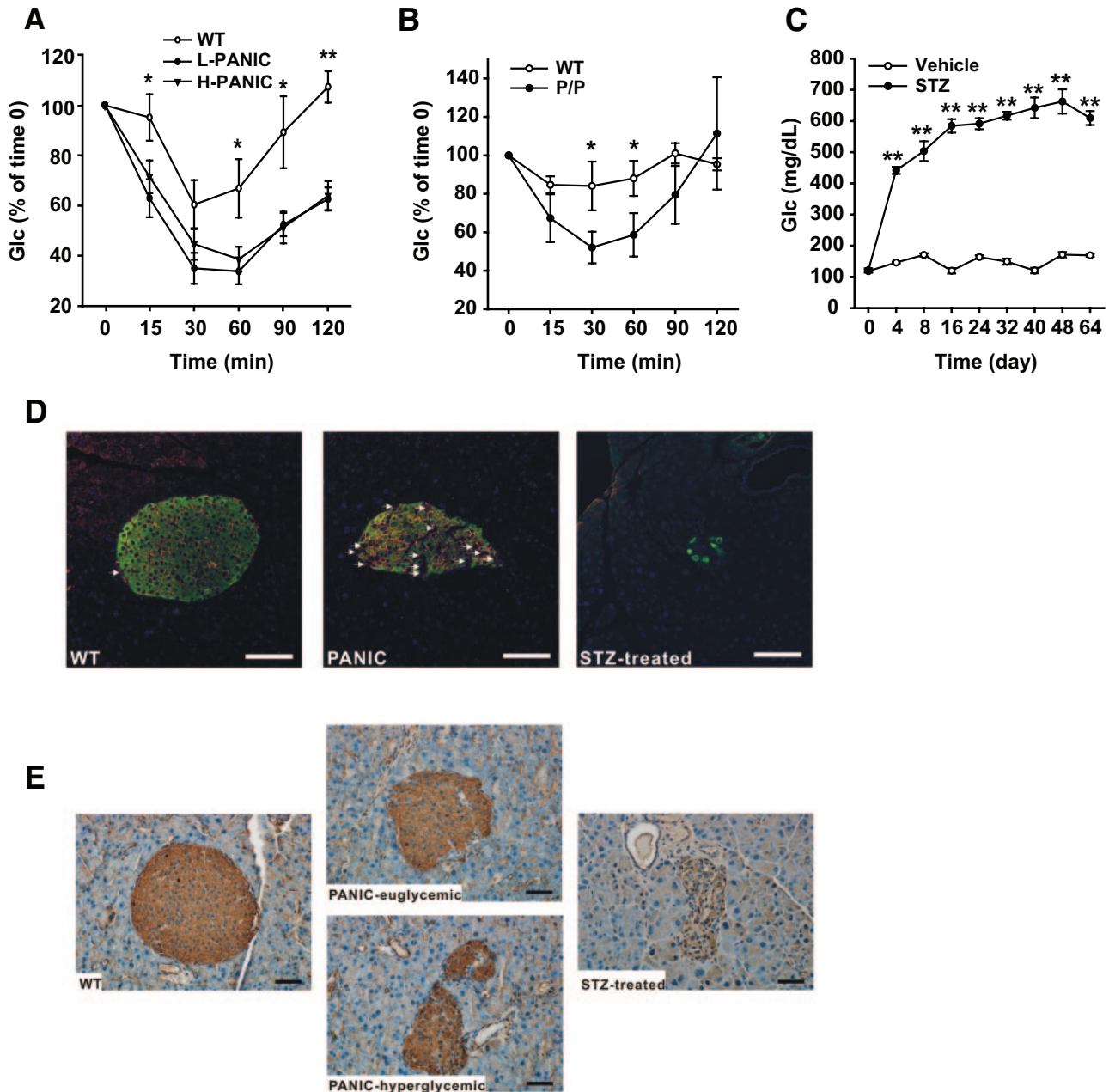


**FIG. 6.** PANIC-ATTAC mice display improved insulin sensitivity and increased population of GLUT2<sup>+</sup>/insulin<sup>-</sup> cells after recovery. **A:** ITT on hemizygous PANIC-ATTAC mice after recovery. Significant differences are seen between wild type vs. low responders (L-PANIC) and wild-type vs. high responders (H-PANIC) at 15, 60, 90, and 120 min. There is no difference between L-PANIC and H-PANIC during the entire course. Wild type, *n* = 3; L-PANIC, *n* = 3; H-PANIC, *n* = 6. \**P* < 0.05, \*\**P* < 0.001. **B:** ITT on homozygous PANIC-ATTAC mice (P/P) after recovery. Significant differences are found between wild-type (*n* = 4) and P/P (*n* = 3) mice at 30 and 60 min. \**P* < 0.05. **C:** Glucose profile of animals administered vehicle and STZ. Vehicle, *n* = 4; STZ, *n* = 5. \*\**P* < 0.001. **D:** Immunofluorescent staining of insulin (green), GLUT2 (red), and nuclei (blue) in recovered homozygous PANIC-ATTAC mice. Arrows indicate GLUT2<sup>+</sup>/insulin<sup>-</sup> cells. Note that there are more GLUT2<sup>+</sup>/insulin<sup>-</sup> cells present in recovered PANIC-ATTAC animals compared with wild-type control mice. In the group administered STZ, very few insulin<sup>+</sup> cells are left, and the islet architecture is disrupted. Scale bar = 50 μm. **E:** Immunohistochemistry staining for GLUT2 in wild-type and homozygous PANIC-ATTAC mice and mice with STZ-induced diabetes. Note that the membrane-bound GLUT2 is restored in the PANIC-euglycemic group, whereas hyperglycemic PANIC-ATTAC mice show intracellular localization of GLUT2 despite the relative normalization of the total signal. Scale bar = 50 μm. (Please see <http://dx.doi.org/10.2337/db07-1631> for a high-quality digital representation of this figure.)

recently, another animal model using inducible Myc activation has been created and characterized, which shows significant regeneration after β-cell ablation (30).

The lack of GSIS in the recovered islets does not come as a surprise. In rat models, hyperglycemia has been reported to cause defective GSIS (19). Additionally, it is possible that the newly differentiated β-cells do not respond to glucose effectively in the recovered islets, presumably because of the lack of a specific factor. Although

it is clear that we fail to fully reconstitute complete functionality of β-cells, this model also represents a unique tool for testing factors and compounds that can confer restoration of GSIS. Putative GSIS reconstitution drugs can be used together with antidiabetes treatments that may only restore the pancreatic insulin content (Figs. 3 and 5). The combination of improvements for both GSIS and pancreatic insulin content is pivotal for effective glyce-mic control. Additionally, this model can also be used to

examine the in vivo effectiveness of candidate genes enabling the restoration of GSIS, which were previously identified in vitro to be critically involved in this process (31).

We have shown a number of “proof of concept” examples of pharmacological interventions that enhance the recovery kinetics on a massive proapoptotic challenge. The PANIC-ATTAC mouse model lends itself for further applications in this area with uniform hyperglycemia and the ability to recover. In the current study, we have used these transgenic mice after hyperglycemia to determine the recovery-enhancing aspects of pharmacological interventions. An equally attractive approach is to test the anti-apoptotic protective mechanisms that may be induced pharmacologically. Using the PANIC-ATTAC mouse model, we are able to screen for pharmacological interventions that confer protective effects on  $\beta$ -cells during diabetes initiation to slow down and prevent the onset of hyperglycemia.

The PANIC-ATTAC mouse model lends itself to additional experimental approaches for which there is currently no experimental paradigm available. Gestational diabetes is associated with adverse effects on fetal development during pregnancy and more importantly, increasing incidence for diabetes in the offspring later in life (32). To study gestational diabetes, glucose infusion and chemical-induced hyperglycemia have been used in animals with limitations and toxin-related complications (33,34). Using PANIC-ATTAC mice, transgene<sup>+</sup> animals can be induced to become hyperglycemic during gestation, exposing wild-type embryos to hyperglycemia without confounding factors. Additionally, to dissect the exact contributions of hyperglycemia in utero versus hyperglycemic effects during lactation on future diabetes development, wild-type pups from diabetic mothers can be adopted by euglycemic mothers and vice versa.

Both neogenesis from precursor cells and replication from adult  $\beta$ -cells have been identified as the mechanism of  $\beta$ -cell regeneration (4,29,35). The inconsistencies may be due to the differences in experimental models and conditions. Here, we define a novel cell population that can be observed at high frequency in recovering PANIC-ATTAC islets. This population is characterized by high level expression of GLUT2, yet these cells have not (or not yet) induced the expression of insulin. We appreciate that we have not formally demonstrated that these cells are precursors for  $\beta$ -cells, and it is possible that they are a curiosity of this particular system. We did not find significant number of GLUT2<sup>+</sup>/insulin<sup>-</sup> cells in wild-type control animals, which argues against this cell population as a resident cell type in islets. However, it is clear that STZ administration at higher concentrations completely eliminates this cell population, and this might be a potential reason to prevent recovery of the islets. The widespread presence of these cells in the recovering PANIC-ATTAC islets is intriguing, but it is also consistent with the finding that GLUT2<sup>+</sup> epithelial cells have been postulated to give rise to adult  $\beta$ -cells during development (36). Additionally, in the ductal ligation model of pancreas injury, increased proliferation of GLUT2<sup>+</sup> cells has been reported in pancreatic ducts (25). We are currently devoting significant efforts toward the isolation of this cell population.

In summary, the PANIC-ATTAC mice provide an inducible model of  $\beta$ -cell loss with the ability of  $\beta$ -cell recovery and a host of novel aspects that most of the previously described pancreas injury models failed to display to date.

Applications of the PANIC-ATTAC mouse model in several areas of islet research may provide an ideal system to improve our understanding of GSIS, gestational diabetes, and the definition of novel  $\beta$ -cell precursors.

#### ACKNOWLEDGMENTS

T.D.S. has received a postdoctoral fellowship from the American Heart Association. P.E.S. has received National Institutes of Health Grant R01-DK-55758 and Juvenile Diabetes Research Foundation (JDRF) Grant 1-2008-16. The work was also supported by JDRF Grant 17-2007-1026 (to Chris Newgard) and TORS Consortium Grant 1PL1DK081182.

We thank Dr. Susan Bonner-Weir (Joslin Diabetes Center) for technical help, instructions, and advice for this project. We thank Yuan Xin (Albert Einstein College of Medicine); Aisha Cordero (Albert Einstein College of Medicine); Virginia Liu, Amy Song, and James Yi (University of Texas); Zhihua Li, Yue Feng, and Yun-Ping Zhou (Merck Research Laboratories) for expert technical assistance; and Nils Halberg (University of Texas and Copenhagen University) for help with the statistical analysis. We thank Ariad Pharmaceuticals for providing the dimerization kit and compound AP20187. We thank Dr. Raymond Macdonald (Department of Molecular Biology, University of Texas Southwestern Medical Center) and Dr. Klaus Kaestner (Department of Genetics, University of Pennsylvania) for providing PDX-1 antibodies. We thank the entire Scherer group for helpful discussions, Dr. Ken Chen and the transgenic core facility at the Albert Einstein College of Medicine for transgenic mouse generation, and the Metabolic Core Facility at University of Texas Southwestern for help in phenotyping. We also thank Drs. Streamson Chua and Jean Herbert from the Albert Einstein College of Medicine for sharing unpublished information.

#### REFERENCES

1. Wild S, Roglic G, Green A, Sicree R, King H: Global prevalence of diabetes: estimates for the year 2000 and projections for 2030. *Diabetes Care* 27:1047–1053, 2004
2. Shapiro AM, Lakey JR, Ryan EA, Korbitt GS, Toth E, Warnock GL, Kneteman NM, Rajotte RV: Islet transplantation in seven patients with type 1 diabetes mellitus using a glucocorticoid-free immunosuppressive regimen. *N Engl J Med* 343:230–238, 2000
3. Lardon J, Huyens N, Rooman I, Bouwens L: Exocrine cell transdifferentiation in dexamethasone-treated rat pancreas. *Virchows Arch* 444:61–65, 2004
4. Bonner-Weir S, Toschi E, Inada A, Reitz P, Fonseca SY, Aye T, Sharma A: The pancreatic ductal epithelium serves as a potential pool of progenitor cells. *Pediatr Diabetes* 5 (Suppl. 2):16–22, 2004
5. Rajagopal J, Anderson WJ, Kume S, Martinez OI, Melton DA: Insulin staining of ES cell progeny from insulin uptake. *Science* 299: 363, 2003
6. Lumelsky N, Blondel O, Laeng P, Velasco I, Ravin R, McKay R: Differentiation of embryonic stem cells to insulin-secreting structures similar to pancreatic islets. *Science* 292:1389–1394, 2001
7. Hao E, Tyrberg B, Itkin-Ansari P, Lakey JR, Geron I, Monosov EZ, Barcova M, Mercola M, Levine F: Beta-cell differentiation from nonendocrine epithelial cells of the adult human pancreas. *Nat Med* 12:310–316, 2006
8. Dor Y, Brown J, Martinez OI, Melton DA: Adult pancreatic beta-cells are formed by self-duplication rather than stem-cell differentiation. *Nature* 429:41–46, 2004
9. Pajvani UB, Trujillo ME, Combs TP, Iyengar P, Jelicks L, Roth KA, Kitsis RN, Scherer PE: Fat apoptosis through targeted activation of caspase 8: a new mouse model of inducible and reversible lipodystrophy. *Nat Med* 11:797–803, 2005
10. Mu J, Woods J, Zhou YP, Roy RS, Li Z, Zychband E, Feng Y, Zhu L, Li C, Howard AD, Moller DE, Thornberry NA, Zhang BB: Chronic inhibition of dipeptidyl peptidase-4 with a sitagliptin analog preserves pancreatic  $\beta$ -cell mass and function in a rodent model of type 2 diabetes. *Diabetes* 55:1695–1704, 2006

11. Meier JJ, Lin JC, Butler AE, Galasso R, Martinez DS, Butler PC: Direct evidence of attempted beta cell regeneration in an 89-year-old patient with recent-onset type 1 diabetes. *Diabetologia* 49:1838–1844, 2006
12. Carley AN, Semeniuk LM, Shimoni Y, Aasum E, Larsen TS, Berger JP, Severson DL: Treatment of type 2 diabetic *db/db* mice with a novel PPAR $\gamma$  agonist improves cardiac metabolism but not contractile function. *Am J Physiol Endocrinol Metab* 286:E449–E455, 2004
13. Kim D, Wang L, Beconi M, Eiermann GJ, Fisher MH, He H, Hickey GJ, Kowalchick JE, Leiting B, Lyons K, Marsilio F, McCann ME, Patel RA, Petrov A, Scapin G, Patel SB, Roy RS, Wu JK, Wyratt MJ, Zhang BB, Zhu L, Thornberry NA, Weber AE: (2R)-4-oxo-4-[3-(trifluoromethyl)-5,6-dihydro[1,2,4]triazolo[4,3-a]pyrazin-7(8H)-yl]-1-(2,4,5-trifluorophenyl)butan-2-amine: a potent, orally active dipeptidyl peptidase IV inhibitor for the treatment of type 2 diabetes. *J Med Chem* 48:141–151, 2005
14. Clackson T, Yang W, Rozamus LW, Hatada M, Amara JF, Rollins CT, Stevenson LF, Magari SR, Wood SA, Courage NL, Lu X, Cerasoli F Jr, Gilman M, Holt DA: Redesigning an FKBP-ligand interface to generate chemical dimerizers with novel specificity. *Proc Natl Acad Sci U S A* 95:10437–10442, 1998
15. Muzio M, Stockwell BR, Stennicke HR, Salvesen GS, Dixit VM: An induced proximity model for caspase-8 activation. *J Biol Chem* 273:2926–2930, 1998
16. Wencker D, Chandra M, Nguyen K, Miao W, Garantziotis S, Factor SM, Shirani J, Armstrong RC, Kitsis RN: A mechanistic role for cardiac myocyte apoptosis in heart failure. *J Clin Invest* 111:1497–1504, 2003
17. Gannon M, Shiota C, Postic C, Wright CV, Magnuson M: Analysis of the Cre-mediated recombination driven by rat insulin promoter in embryonic and adult mouse pancreas. *Genesis* 26:139–142, 2000
18. Laybutt DR, Glandt M, Xu G, Ahn YB, Trivedi N, Bonner-Weir S, Weir GC: Critical reduction in beta-cell mass results in two distinct outcomes over time: adaptation with impaired glucose tolerance or decompensated diabetes. *J Biol Chem* 278:2997–3005, 2003
19. Bonner-Weir S, Trent DF, Weir GC: Partial pancreatectomy in the rat and subsequent defect in glucose-induced insulin release. *J Clin Invest* 71:1544–1553, 1983
20. Shimabukuro M, Zhou YT, Levi M, Unger RH: Fatty acid-induced beta cell apoptosis: a link between obesity and diabetes. *Proc Natl Acad Sci U S A* 95:2498–2502, 1998
21. Goke R, Fehmann HC, Linn T, Schmidt H, Krause M, Eng J, Goke B: Exendin-4 is a high potency agonist and truncated exendin-(9–39)-amide an antagonist at the glucagon-like peptide 1-(7–36)-amide receptor of insulin-secreting beta-cells. *J Biol Chem* 268:19650–19655, 1993
22. Xu G, Stoffers DA, Habener JF, Bonner-Weir S: Exendin-4 stimulates both  $\beta$ -cell replication and neogenesis, resulting in increased  $\beta$ -cell mass and improved glucose tolerance in diabetic rats. *Diabetes* 48:2270–2276, 1999
23. Rosen ED, Kulkarni RN, Sarraf P, Ozcan U, Okada T, Hsu CH, Eisenman D, Magnuson MA, Gonzalez FJ, Kahn CR, Spiegelman BM: Targeted elimination of peroxisome proliferator-activated receptor gamma in beta cells leads to abnormalities in islet mass without compromising glucose homeostasis. *Mol Cell Biol* 23:7222–7229, 2003
24. Brunham LR, Kruit JK, Pape TD, Timmins JM, Reuwer AQ, Vasanji Z, Marsh BJ, Rodrigues B, Johnson JD, Parks JS, Verchere CB, Hayden MR: Beta-cell ABCA1 influences insulin secretion, glucose homeostasis and response to thiazolidinedione treatment. *Nat Med* 13:340–347, 2007
25. Wang RN, Kloppel G, Bouwens L: Duct- to islet-cell differentiation and islet growth in the pancreas of duct-ligated adult rats. *Diabetologia* 38:1405–1411, 1995
26. Schnedl WJ, Ferber S, Johnson JH, Newgard CB: STZ transport and cytotoxicity: specific enhancement in GLUT2-expressing cells. *Diabetes* 43:1326–1333, 1994
27. Orzi L, Ravazzola M, Baetens D, Inman L, Amherdt M, Peterson RG, Newgard CB, Johnson JH, Unger RH: Evidence that down-regulation of beta-cell glucose transporters in non-insulin-dependent diabetes may be the cause of diabetic hyperglycemia. *Proc Natl Acad Sci U S A* 87:9953–9957, 1990
28. Herrera PL, Huarte J, Zufferey R, Nichols A, Mermillod B, Philippe J, Muniesa P, Sanvito F, Orzi L, Vassalli JD: Ablation of islet endocrine cells by targeted expression of hormone-promoter-driven toxigenes. *Proc Natl Acad Sci U S A* 91:12999–13003, 1994
29. Nir T, Melton DA, Dor Y: Recovery from diabetes in mice by beta cell regeneration. *J Clin Invest* 117:2553–2561, 2007
30. Cano DA, Rulifson IC, Heiser PW, Swigart LB, Pelengaris S, German M, Evan GI, Bluestone JA, Hebrok M: Regulated  $\beta$ -cell regeneration in the adult mouse pancreas. *Diabetes* 57:958–966, 2008
31. Schisler JC, Jensen PB, Taylor DG, Becker TC, Knop FK, Takekawa S, German M, Weir GC, Lu D, Mirmira RG, Newgard CB: The Nkx6.1 homeodomain transcription factor suppresses glucagon expression and regulates glucose-stimulated insulin secretion in islet beta cells. *Proc Natl Acad Sci U S A* 102:7297–7302, 2005
32. Dabelea D, Pettitt DJ: Intrauterine diabetic environment confers risks for type 2 diabetes mellitus and obesity in the offspring, in addition to genetic susceptibility. *J Pediatr Endocrinol Metab* 14:1085–1091, 2001
33. Aerts L, Van Assche FA: Animal evidence for the transgenerational development of diabetes mellitus. *Int J Biochem Cell Biol* 38:894–903, 2006
34. Hay WW Jr: Recent observations on the regulation of fetal metabolism by glucose. *J Physiol* 572:17–24, 2006
35. Teta M, Rankin MM, Long SY, Stein GM, Kushner JA: Growth and regeneration of adult beta cells does not involve specialized progenitors. *Dev Cell* 12:817–826, 2007
36. Pang K, Mukonoweshuro C, Wong GG: Beta cells arise from glucose transporter type 2 (Glut2)-expressing epithelial cells of the developing rat pancreas. *Proc Natl Acad Sci U S A* 91:9559–9563, 1994